International Journal of Geosynthetics and Ground Engineering (2023) 9:1
https://doi.org/10.1007/s40891-022-00421-y

CASE STUDY

Properties of HDPE Geomembrane Exhumed 20 Years After Installation in a Mine Reclamation Cover System

Ramanambelina Faneva Mamambina Rarison[1] · Mamert Mbonimpa[1] · Bruno Bussière[1] · Sandra Pouliot[2]

Received: 19 September 2022 / Accepted: 27 November 2022
© The Author(s), under exclusive licence to Springer Nature Switzerland AG 2022

Abstract
High-density polyethylene (HDPE) geomembranes (GM) are used in mine site reclamation cover systems to limit water and oxygen ingress into sulphide tailings or waste rocks, thereby reducing acid mine drainage generation. The objective of this paper is to assess the actual properties of small-scale GMs after 20 years of service in the cover system of an existing mine site. GM samples were exhumed from this site and laboratory tested to determine the standard (*Std*) and high pressure (*HP*) oxidative-induction times (*OITs*), tensile properties, and hydraulic and oxygen sorption/diffusion properties. Unfortunately, the initial properties of the virgin GM before the installation were not available. Properties gathered from this study were then compared to literature data or to minimal requirements for virgin HDPE GMs as defined by the Geosynthetic Research Institute (GRI). Results showed Std-OIT values exceeding the minimum requirement of 100 min for virgin GMs while the *HP-OIT* values are lower than the minimum requirement of 400 min. The tensile properties exceed the requirements. The fluid-tightening properties do not appear to be affected to date: the equivalent hydraulic conductivity is around 10^{-14} m/s, and the oxygen diffusion coefficient is around 10^{-13} m^2/s. The GMs thus show acceptable performance to date. Further studies will be needed in the future to determine more long-term GM behaviour where the data from this study will constitute reference values (in the absence of initial properties).

Keywords Geosynthetics · Geomembrane · Mine site reclamation · Cover system · Exhumation · *OIT* · Tensile · Fluid transport properties

Introduction

Mine sites generate substantial amounts of wastes that must be carefully managed and/or treated to prevent environmental impacts to the surrounding ecosystem. When sulphide tailings and waste rocks are stored in surface impoundments, this challenge becomes greater. Indeed, when such sulphide wastes are in contact with water and oxygen, acid mine drainage (AMD) can be generated in the absence of enough neutralization capacity. AMD is characterized by acidic pH (typically from 2 to 5) with high concentrations of dissolved metals and sulphate, which can be environmentally damaging [1, 2].

In recent decades, various techniques have been developed to control AMD production in surface waste impoundments [3]. One reclamation solution for acid-generating tailings is to apply a multilayered cover system, as illustrated in Fig. 1, to limit the ingress of water and/or oxygen to the tailings beneath [4–7]. A typical multilayered cover may contain up to five layers. From top to bottom, it includes: (1) a surface layer to allow transition between the atmosphere and the underlying layers and to provide support for vegetation, thereby preventing erosion; (2) a protection layer to prevent bio-intrusion; (3) a drainage layer to control lateral and vertical water inflow and prevent water evaporation from the underlaying layer (fluid barrier layer); (4) a fluid barrier

✉ Ramanambelina Faneva Mamambina Rarison
faneva.rarison@uqat.ca

Mamert Mbonimpa
mamert.mbonimpa@uqat.ca

Bruno Bussière
bruno.bussiere@uqat.ca

Sandra Pouliot
sandra.pouliot@snclavalin.com

[1] Research Institute On Mines and the Environment, Université du Québec en Abitibi-Témiscamingue, 445 Boul. de L'Université, Rouyn-Noranda, Québec J9X 5E4, Canada

[2] Mining and Metallurgy, SNC-Lavalin, 1271 7e Rue, Val-d'Or, Québec J9P 3S1, Canada

Published online: 10 December 2022

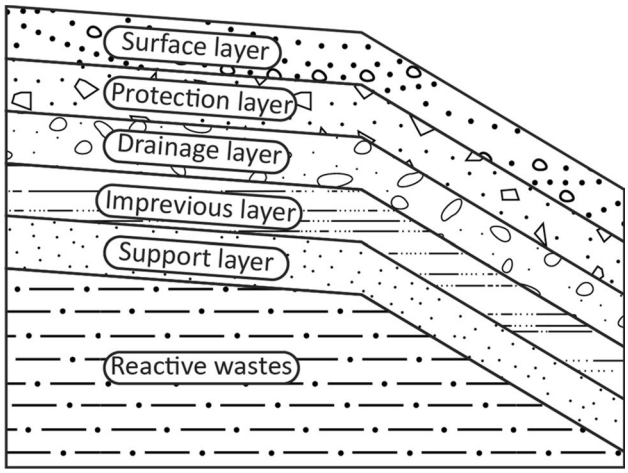

Fig. 1 Configuration of a typical multilayered cover system adapted from Aubertin et al. [4]

layer, which is critical for controlling water and/or oxygen ingress; and (5) a support layer placed directly on the tailings to bear the overlying layers [4].

The different layers can be composed of natural soil and/or alternative materials, depending on the cover's main function (oxygen or water/hydraulic barrier). In the case of low saturated hydraulic conductivity covers, layer D consists of materials with low saturated hydraulic conductivity (k_{sat}) such as fine-grained soils (clay or fine silt), geomembranes (GMs), geosynthetic clay liners (GCL), soil-bentonite mixes, or a combination of these [4, 5, 8]. Typical k_{sat} values for layer D are below 10^{-9} m/s [4].

GMs are synthetic materials composed of resin, used as a matrix, and additives to provide protection and specific properties [9, 10]. Resin is prone to oxidation, leading to material degradation and photodegradation. Oxidation causes carbonyl group formation, which indicates the GM degradation stage. Hence, GMs require the inclusion of antioxidants and stabilizers (AO/S) to protect against oxidation and carbon black to protect against exposure to ultraviolet (UV) [10–12]. Because AO/S deplete over time, AO/S levels are determined to indicate the GM degradation stages, as conceptualized by Hsuan and Koerner [13]. In Hsuan and Koerner's conceptual degradation model, the GM ageing process is considered as a three-stage process: depletion of antioxidants and stabilizers (stage 1); induction time (stage 2) up to a significant drop in the GM properties (indicating the onset of stage 3); and polymer degradation (stage 3) up to a 50% drop in GM properties (based on GM initial properties).

Among a variety of GM types, high-density polyethylene (HDPE) GM is the most widely used worldwide [9, 10, 14, 15], and particularly for mine site reclamation covers, including at 11 of 12 sites found in the literature [16, 17]. Those HDPE GMs were widely used as they have a better chemical resistance, and they were relatively inexpensive compared to others, for example linear low-density polyethylene GMs [10]. However, the chemical concern did not apply for well-designed cover so that the GM is not in direct contact with tailings. The 12 cover configurations are summarized in Table 1. For all the 12 sites, 8 smooth 1.5 mm-thick HDPE GMs, 1 smooth 0.75 mm-thick HDPE GM, 2 textured 1.5 mm-thick HDPE GMs, and one smooth 1 mm-thick linear low-density polyethylene (LLDPE) GM was used. Textured GMs were installed on the slopes to ensure better slope stability, as the soil/textured GM friction properties increased compared to smooth GMs [9, 10, 14, 15]. It is usually accepted that textured GMs would have shorter service life than smooth ones. This is due to surface corrugations that allow greater exposure to the surrounding media, resulting in faster AO evaporation/dissolution from the GM surface [18]. In two cases reported in the literature (Normetal and Mid-North sites), the GMs were also in direct contact with AMD-contaminated interstitial water, which could reduce the GM lifetime. Accordingly, Gulec et al. [19–21] and Rarison [16] estimated faster degradation when the GM was in contact with AMD than non-contaminated water.

The majority of the sites listed in Table 1 are located in cold regions of Canada. Cold region is defined as an area where the permafrost is continuous or discontinuous (causing seasonal thawing in the active layer) or where the frost depth exceeds at least 0.3 m (causing seasonal freezing in layers having thickness less than the frost depth) [22–25]. In the Abitibi-Témiscamingue region where two sites were reclaimed with HDPE GMs (cf. Table 1), the frost depth can reach 2.0 m in the absence of any snow cover [16, 26]. Given the thicknesses of the overlying cover layers, GMs could be prone to seasonal thawing in the summer when permafrost is present (e.g., at the Raglan experimental cell) or seasonal freezing in the winter when frost penetrates (e.g., at the Weedon, Normetal, and Victoria Junction sites). Cold temperatures slow the oxidation reaction according to Arrhenius' law, and consequently the GM degradation rate [27–29]. Previous results on laboratory tested specimens [16] show that freeze–thaw cycling (up to 300 daily cycles) alone would have no significant adverse effect on the GM mechanical, hydraulic, or oxygen sorption and diffusion properties, as found by others for mechanical [10, 30–32] and diffusion properties [33].

Nevertheless, little is known about the in-situ behaviour of GMs used for the reclamation of mine waste storage facilities. Therefore, the adverse effects of AMD and cold temperature (with seasonal freezing) on GMs used in mining cover systems remain to be investigated. One way to assess these effects is to exhume GMs from existing cover systems. GM exhumation is commonly used for in-service performance assessment. For example, exhumed GMs were

Table 1 Mine sites reclaimed with cover systems that include GMs, presented chronologically by reclamation years, adapted from Mbonimpa et al. [17]

Site (location)	Type of waste	Reclamation year	Downward cover structure	References
Weedon (Eastern Townships, Québec, Canada)	Tailings	1993	• 0.3 m-thick topsoil • 0.7 m-thick sand • 1.5 mm-thick HDPE GM • Sand and gravel	[62]
Kwinana (Western Australia, Australia)	Tailings	1998	• 2–4 m-thick sand • 0.75 mm-thick HDPE GM • 7.2 mm-thick bentonite geocomposite • 2 m-thick sand	[63]
Mid-North (North of Québec, Québec, Canada)[a]	Tailings	1999–2000	• 1.35 m-thick till • 1.5 mm-thick HDPE GM	[42, 43]
Normetal (Abitibi-Témiscamingue, Québec, Canada)	Tailings	2005–2006	• 0.6 m-thick silt • 1.5 mm-thick HDPE GM	[64]
Victoria Junction (Cape Breton, Nova Scotia, Canada)	Waste rock	2006	• 0.4 m-thick till • 0.4 m-thick granular drain layer • 1.5 mm-thick HDPE GM • 0.15 mm-thick sand	[65–68]
Eustis (Eastern Townships, Québec, Canada)	Tailings	2007–2008	• 0.10 m-thick topsoil • 0.50 m-thick deinking residues • Geodrain • 1.5 mm-thick textured HDPE GM • 0.3 m-thick sand	[69–71]
	Waste rock	2008–2009	• 0.10 m-thick topsoil • 0.50 m-thick deinking residues • Geodrain • 1.5 mm-thick textured HDPE GM • Geotextile	
Aldermac, south sector (Abitibi-Témiscamingue, Québec, Canada)	Tailings	2008–2009	• 1-m thick sand and gravel • Geotextile • 1.5 mm-thick textured HDPE GM • 0.30 m-thick sand and grave	[71–74]
Scotchtown Summit (Cape Breton, Nova Scotia, Canada)	Waste rock	2009–2011	• 0.5 m-thick till • Geotextile • 1.5 mm-thick HDPE GM • 0.15 m-thick sand	[67, 75]
Franklin (Cape Breton, Nova Scotia, Canada)	Waste rock	2010	• 0.6 m-thick till • Drainage-net • 1.5 mm-thick HDPE GM • Geofabric	[67, 76, 77]
Barvue (Abitibi-Témiscamingue, Québec, Canada)	Tailings	2014	• 0.12 m-thick topsoil • 0.40 m-thick loamy sand soil • 0.70 m-thick sand and gravel • 0.30 m-thick sand • 1.5-mm thick HDPE GM • 0.30 m-thick sand • 0.40 m-thick sand and gravel	[71, 78]
Suffield (Eastern Townships, Québec, Canada)	Tailings	2015	• 0.12 m-thick topsoil • 0.40 m-thick loamy sand and soil • 0.40 m-thick sand and gravel • 0.30 m-thick sand • 1.0 mm-thick LLDPE GM • 0.30 m-thick sand • 0.30 m-thick sand and gravel	[71]
Raglan experimental cell (Nunavik, Québec, Canada)	Tailings	2012	• 0.60 m-thick riprap • 0.40 m-thick crushed rock • 1.5 mm-thick HDPE GM • 0.40 m-thick crushed rock	[79]

[a]The name of this site has been changed for confidentiality reasons

used to assess: (1) the stress-cracking resistance of 7 HDPE GMs exhumed from bottom liners with different exposure times ranging from less than a year up to 10 years [34]; (2) the tensile properties of HDPE GM field waves exhumed from a municipal solid waste landfill after 8 years of service [35]; (3) the durability of fluorinated HDPE GMs exhumed from a composite barrier constructed for hydrocarbons spill containment based on samplings after 1, 3, 6, and 7 years of service [36]; (4) the properties of geosynthetics (HDPE geocomposite drain, LLDPE GM, and geosynthetic clay liner) in landfill covers after 4.7 to 5.8 years of service [37]; (5) the long-term performance of an HDPE GM liner in a water reservoir [38]; and (6) the long-term performance of geosynthetics (geosynthetic clay liners, HDPE GMs, and geotextiles) in composite barrier systems for hydrocarbon-contaminated soil remediation [39, 40]. The properties of exhumed GMs are then compared to initial values, if available, or to literature values such as the GRI GM13 [41] requirements for HDPE GM, depending on the properties of interest. In addition, the antioxidant/stabilizer level is usually assessed to characterize the GM degradation stage according to Hsuan and Koerner [13] oxidation degradation model.

This paper assesses the properties of a 20-year-old HDPE GM used in a low saturated hydraulic conductivity covers applied for mine site reclamation to limit water and oxygen ingress into sulphide tailings. GM samples were exhumed from two areas where the GM is supposed to be unstrained and strained, respectively. In addition to chemical analyses to determine the GM degradation stage, three key parameters were determined on exhumed GMs: tensile properties to assess the mechanical properties, permeability to assess the sealing capacity, and oxygen sorption and diffusion properties to assess the ability to limit oxygen flux. Unfortunately, the initial properties of the virgin GM before the installation were not available which does not allow to assess the evolution of the different properties over the 20 years of service. For this reason, the actual properties are compared to literature data or to GRI GM13 [41] minimal requirements for virgin HDPE GMs. The results presented in this paper will serve for comparison purpose with data gathered from future studies.

Geomembrane Exhumation

The GMs were exhumed from a site in the Mid-North region (site MN), reclaimed in 2000 with a cover including a smooth 1.5 mm-thick HDPE GM. Figure 2 illustrates the configuration of the reclamation cover. The GM is located at depths of 1.35 m. Knowing that the potential frost depth could reach 2.0 m in the region [16, 26], the GM could undergo seasonal freezing. The GM is in direct contact with oxidized tailings (see Table 1 and Fig. 2). As mentioned

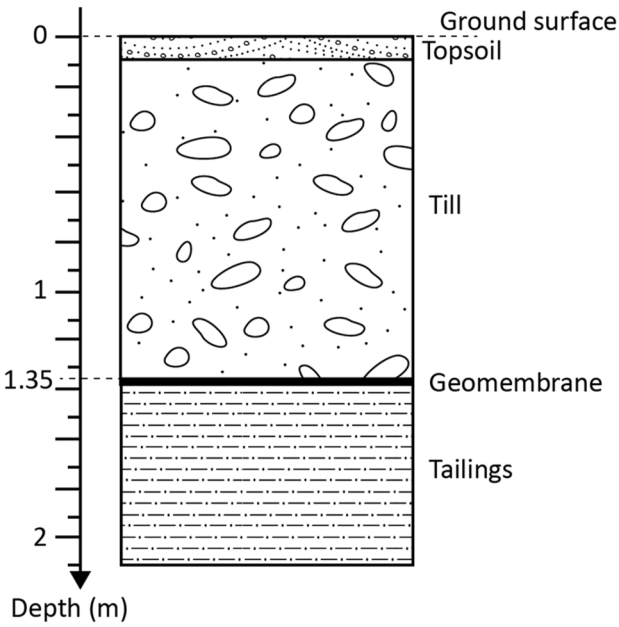

Fig. 2 Configuration of the cover system at the MN site

earlier, this represents the worst-case scenario due to AMD effects on GM degradation [16, 19–21].

Historically, the geometry of the site was like a dome [42] but settlements of about 40 to 47 cm were measured at the centre of the dome during the first years [43] leading to a new geometry with a depression zone in the centre. The settlements could be problematic as they induce permanent tensile stress into the GM that could generate GM thinning and then an accelerated degradation [44], even cracks [34]. To assess the effect of the settlement, GM sampling was carried out approximately in the middle of the depression where the GM is supposed to be unstrained (noted U), and at the side of the depression zone where the GM is supposed to be strained (noted S). The geographical coordinates of the exhumation areas in terms of DMS Lat and DMS Long are N49°26′43″ and W78°23′53.5″ for the unstrained area and N49°26′37.7″ and W78°24′10.2″ for the strained area, respectively (see Table 2).

The GM exhumation was performed in August 2020. The exhumation can be summarized in four steps: (1) stripping, (2) excavation and GM cleaning, (3) GM sampling, and (4) material replacement and rehabilitation. More specifically, the exhumation campaign began with a delimitation of the work area to obtain a work surface of 4 m × 4 m at the depth of the GM. Because vegetation was present on the surface, stripping was done with care to preserve the excavated soil in the form of vegetation-covered tiles. The tiles were replaced after exhumation to facilitate vegetation recovery. Once the protective layer was laid bare, excavation was performed using a mechanical shovel, with care when approaching

Table 2 Properties of virgin GM versus GM exhumed from the MN site

Properties (units)	Virgin	Mid-North site			
		Unstrained		Strained	
		MD	CD	MD	CD
Age (years)	0	20			
Geographical coordinates	–	N49°26′43” W78°23′53.5”		N49°26′37.7” W78°24′10.2”	
Physical					
T_{GM} (mm)	1.5[a]	1.566		1.539	
Chemical					
Std-OIT (min)	> 100[b]	102		120	
HP-OIT (min)	> 400[b]	301		326	
Tensile					
TYS (N/mm)	> 22[b]	28.3	28.6	27.9	28.4
PYE (%)	> 12[b]	17.4	17.4	17.7	16.4
TBS (N/mm)	> 40[b]	66.0	64.8	60.6	60.3
PBE (N/mm)	> 700[b]	1008	998	910	940
Hydraulic					
K_g (m/s)	$[1.10\times10^{-15};1.12\times10^{-14}]$[c]	2.9×10^{-14}		1.3×10^{-14}	
Oxygen partition coefficient S_g (-)	–	13.38		13.19	
Oxygen diffusion coefficient D_g (m^2/s)	$[1.79\times10^{-11};3.59\times10^{-11}]$[d]	1.50×10^{-13}		1.40×10^{-13}	
Oxygen permeation coefficient P_g (m^2/s)	–	2.01×10^{-12}		1.85×10^{-12}	

[a]Nominal thickness

[b]Minimum values according to GRI GM13[41]

[c]According to Haxo Jr et al. [59] and Giroud and Bonaparte[51]

[d]According to Massey [60] and Wagner Jr [61] (for HDPE films)

the GM. Closer to the GM, cleaning was performed with a manual shovel to prevent damage to the GM. The GM was then cleaned with fresh water to reveal its general state. On visual inspection, some waves were observed, but no major defects were noted. Figure 3 shows some photographs taken during the exhumation.

GM sampling was then performed. A sample was taken from the exhumed GM (U and S) using a cutter with a frame

Fig. 3 Photographs taken during the exhumation: **a** excavation, **b** cleaning and **c** GM sampling

to obtain square 1 m × 1 m sheet. Once the sampling was completed, the GMs were replaced by a contractor certified by the International Association of Geosynthetics Installers to ensure the integrity of the covers. The protective layers were then immediately replaced at similar state than before the exhumation along with the vegetation-covered topsoil tiles. The GM samples were then cleaned with fresh water on site and transported to the laboratory where they were stored and protected from UV rays to prevent degradation. The sheet samples were then used to perform physical, chemical, mechanical, hydrogeological, and oxygen diffusion characterization tests. The direction in which the GM roll was installed (machine direction, MD) was also marked to allow assessing potential GM anisotropy by comparing tensile properties in MD and crossmachine direction (CD).

Geomembrane Characterization Methods

Geomembrane Thickness

The thickness of the GM samples was measured according to ASTM D5199 [45] using an MTG-DX2 thickness gauge which has an accuracy of ± 4 µm (Checkline, USA). The GM thickness T_{GM} was defined as the mean of 10 thickness measurements on 80 mm diameter disks.

Antioxidant/Stabilizer Levels

The antioxidant and stabilizer levels were assessed by differential scanning calorimetry (DSC) according to the standard (*Std-OIT*) and high-pressure oxidative-induction time (*HP-OIT*) methods described in ASTM D3895 [46] and D5885 [47], respectively. The *Std-OIT* were performed in-house using a STD Q600 TGA/DSC analyzer (T.A. Instruments, US) at 200 ℃, and the *HP-OIT* were performed by an external lab (SAGEOS GCTT Group, QC, Canada) at 150 ℃ under a pressure of 3.4 MPa. The standard tests were performed in duplicate, and the high-pressure tests were only performed with single scanning on the U and S samples. The two tests are complementary as the effective temperature ranges of antioxidants and stabilizers are different. For example, hindered phenols, whose effective temperature range is up to 300 ℃, can be detected with the standard test, while hindered amines, whose effective temperature range is up to 150 ℃, can only be detected with the high-pressure test [10, 13].

Tensile Tests

The tensile properties of the exhumed GMs were assessed by tensile testing according to ASTM D6693 [48] at a test speed of 50 mm/min. For each U and S GMs, specimens were prepared in the two principal directions: in machine direction (MD) and in crossmachine direction (CD). Five tests were performed for each direction. The tests were performed with a BT1-FR020TN tensile bench (Zwick Roell GmbH, Germany). Each test gives the stress–strain curves for the determination of four parameters: the tensile yield strength (*TYS*), the percent yield elongation (*PYE*), the tensile break strength (*TBS*), and the percent break elongation (*PBE*).

Permeability Tests

Single permeability tests were performed on the U and S GMs using an in-house setup according to the European standard NF EN 14150 [49]. Each test takes about 20 days. Details of the setup and method are presented in Rarison et al. [50]. In summary, the GM specimen (24 cm in diameter) is placed between two half cells, one upstream and one downstream, which are then filled with deaerated water keeping a pressure difference Δp of 100,000 Pa between the upstream and downstream side of the GM. The pressure and volume in the two half cells are monitored by a VJT2267 dual automatic hydraulic pressure/volume controller (VJ Tech, United Kingdom). The test provides the volumetric flux of deaerated water (Q) through the GM per unit of time. The equivalent hydraulic conductivity K_g (m/s) can be then determined from Q (m^3/s) with mathematical transformations of the equation developed by Giroud and Bonaparte [51] (see Eq. 1):

$$K_g = \frac{Q \times \rho_w \times g \times T_{GM}}{\Delta p \times A}, \quad (1)$$

where ρ_w is the density of the deaerated water used with $\rho_w = 995.67$ kg/m^3 at 30 ℃ [52] (where 30 ℃ is the water temperature recorded by the pressure/volume controller), g is the acceleration due to gravity (9.81 m/s^2), T_{GM} is the GM thickness (m) as determined with ASTM D5199 [45], Δp is the pressure difference (100,000 Pa), and A is the surface area (m^2) of the GM specimen. The area A corresponds to a disc surface for the internal diameter (20 cm) of the cell, where $A = 0.0314$ m^2.

Preliminary permeability tests (five tests) were conducted to evaluate the equivalent hydraulic conductivities of a typical virgin HDPE GMs with a thickness of 1.5 mm. Results were used to determine the standard error of the measurement. A mean K_g of 1.10×10^{-14} m/s with a standard deviation of 4.50×10^{-15} m/s were obtained. This standard deviation was then used to calculate the standard error of the measurement which was applied on the

results obtained from the single test performed on the U and S GMs.

Oxygen Sorption and Diffusion Tests

The oxygen mass flux through a GM sheet can be given by Eq. (2) [53]:

$$f = -D_g \frac{dC_g}{dz} = -S_{gf} D_g \frac{dC_f}{dz} = -P_g \frac{dC_f}{dz}, \quad (2)$$

where f is the oxygen flux (kg/m^2/s), D_g is the oxygen diffusion coefficient (m^2/s), C_g is the oxygen concentration in the geomembrane (kg/m^3), z is the oxygen diffusion direction (m), S_{gf} is the oxygen partition coefficient (-), C_f is the oxygen concentration in the fluid, and P_g is the oxygen permeation coefficient (m^2/s).

The oxygen sorption and diffusion properties of the GM are determined using in-house sorption and diffusion testing setups [16] to obtain S_{gf} and D_g, respectively. P_g is then determined with Eq. 2. For each U and S GM, a sorption test was performed using a sorption cell in which the two half-chambers were filled with pure oxygen. S_{gf} is then determined at equilibrium with the following mathematical transformation of the equation developed by Sangam and Rowe [53]:

$$S_{gf} = \frac{(C_{f0} - C_{fF}) H_{\text{cell}}}{C_{fF} T_{\text{GM}}}, \quad (3)$$

where C_{f0} is the initial oxygen concentration, C_{fF} is the oxygen concentration at equilibrium, H_{cell} is the half-cell height(m), and T_{GM} is the GM thickness (m).

Simultaneously with each sorption test, a diffusion test was performed with a diffusion cell in which the source chamber is filled with pure oxygen and the receptor chamber is filled with pure nitrogen. During the test, the oxygen concentration in the source chamber decreases while the oxygen concentration in the receptor chamber increases. POLLUTE V. 7 software [54] is then used to interpret the test results to obtain D_g. Each simultaneous sorption and diffusion test takes about 30 days. The test is described in greater detail in Rarison, et al. [50]. Preliminary tests have given mean D_g of 5.75×10^{-13} m^2/s with a standard deviation of 4.8×10^{-13} m^2/s for virgin HDPE GMs with a thickness of 1.5 mm. These preliminary tests were also used to define the standard error of the measurement related to the single test performed on the U and S GMs.

Statistical Analysis

To assess the significance of the differences between the results from the unstrained and strained zones or the machine and crossmachine directions, two-sample t tests [55] have been carried out. A two-sample t test is a statistical analysis for mean comparison of two sets of data from a normal distribution. This test is used to distinguish whether the means of two groups (inter-group variation) are significantly different or not, considering the intra-group variation. The test gives a p value that should be superior to the significance level to verify if the means are not significantly different. The normality of the distributions have been verified with Kolmogorov–Smirnov test [56]. The p value given by this normality test should be superior to the significance level to verify the normality of the distribution. The statistical analysis has been performed with OriginPro software. Those tests work for small size samples ($n \geq 3$). The significance level has been set to 0.05 for those tests. They have been used to assess the significance of the differences between the results for the thickness of U and S GMs, and the tensile properties of U and S GMs in MD and CD.

Results and Discussions

Table 2 summarizes the different properties of virgin GM (from the literature) and the measured properties.

Geomembrane Thickness

Figure 4 shows box plots (with standard deviation as error bars) of the measured thicknesses T_{GM} of unstrained and strained GM specimens. The mean thicknesses are 1.566 mm and 1.539 mm for the unstrained and strained GM, respectively (see Table 2). These values are above the nominal thickness of 1.5 mm. Furthermore, T_{GM} from the unstrained GM are higher than the strained. After the verification of

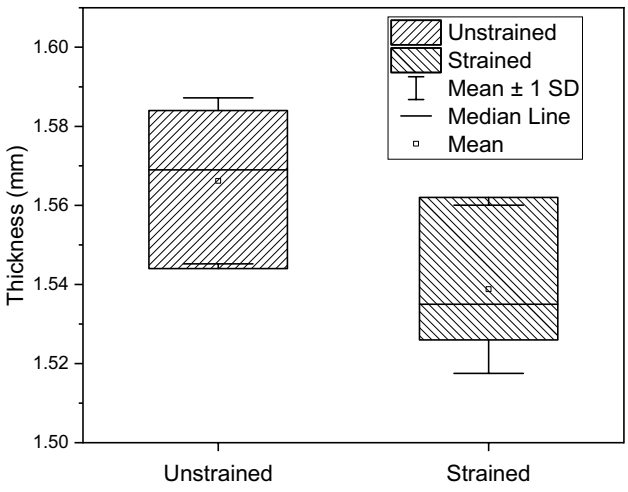

Fig. 4 Box plots (with standard deviation as error bars) of the thicknesses of unstrained and strained GMs

the normality of the data distribution (p value($T_{GM\text{-}U}$) = 0.94 and p value($T_{GM\text{-}S}$) = 0.86), two-sample t test showed that the mean difference between T_{GM} of the unstrained and strained GM is significative (p value($T_{GM\text{-}U}$ vs. $T_{GM\text{-}S}$) = 0.01), which means that the settlement appears to induce GM thinning.

Antioxidant/Stabilizer Levels

The standard (*Std*) and high pressure (*HP*) *OITs* of the unstrained and strained GMs are shown in Fig. 5 and presented in Table 2. The mean *Std-OITs* are 102 min and 120 min and the *HP-OITs* are 301 min and 326 min for GMs exhumed from the unstrained and strained areas, respectively. The unstrained GM has then lower quantity of AO/S compared to the strained GM which means that the unstrained GM is more degraded than the strained one. The difference could be due to the heterogeneity of the tailings, and then the media to which the GM is exposed to. The tailings in the centre of the impoundment where the U GM was exhumed were highly oxidized [42] and would then be more aggressive than the tailings in the edge of the impoundment where the S GM was exhumed, leading to the reduction of *OITs*. Indeed, the tailings in the edge of the impoundment were partly or non-oxidized [42]. It could be also due to the water accumulation in the centre of the impoundment where the U GM was exhumed.

The *Std-OITs* exceed the minimum requirement of 100 min, while the *HP-OITs* are lower than the minimum requirement of 400 min for virgin HDPE GMs, according to GRI GM13 [41]. The degradation of *HP-OIT* could indicate that the GM would have been exposed to atmospheric condition for a long time before the installation of the overlying till layer, leading to the depletion of hindered amine light stabilizers.

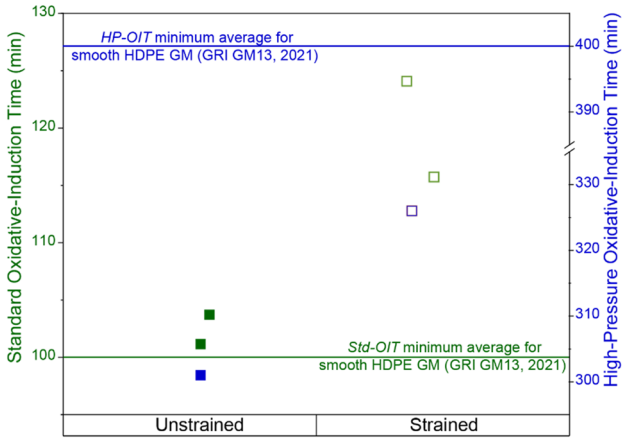

Fig. 5 Standard and high-pressure OITs of unstrained and strained GMs

When the *OITs* reaches a plateau corresponding to their residual values, the antioxidants and stabilizers would be completely depleted [13, 57]. These residual values can be as low as 1.5 min and 80 min for *Std-OIT* and *HP-OIT*, respectively, depending on the antioxidant/stabilizer package, according to Ewais, et al. [58]. There has certainly been AO/S depletion other the 20 years of service, but the GMs still contain AO/S as the OITs are largely above the typical residual values mentioned by Ewais, et al. [58]. The GMs then remain in the antioxidant depletion stage according to Hsuan and Koerner [13] degradation model. The loss of AO/S from the GM would change the structure of the amorphous zone. That could then affect the tensile properties and especially the permeability and the oxygen diffusion properties.

Tensile Properties

The results for the tensile properties in machine direction (MD) and crossmachine direction (CD) are presented as box plots in Fig. 6, depicting the yield properties (*TYS* and *PYE*) and break properties (*TBS* and *PBE*). The obtained mean tensile properties are presented in Table 2 and compared to the minimum requirements for virgin HDPE GM according to GRI GM13 [41] (see Fig. 6). The first observation is that, all the tensile properties exceed the minimum requirements for smooth HDPE GM with a thickness of 1.5 mm [41] which means that the exhumed GMs have decent tensile properties to be used as they should.

The results of the normality verification are presented in Table 3 and the results of the mean comparison are presented in Table 4. There are no statistically significant differences between the results from MD and CD for a given exhumation area (strained or unstrained GM specimens), which means that there is no anisotropy of the tensile properties of the material, with the exception, however, of the *PYE*. Furthermore, there are no significant differences between the yield properties of the samples from unstrained and strained areas for a given direction, which means that the settlement has no significant effect on the yield properties. For example, the *TYS* for the exhumed unstrained and strained GMs are 28.3 and 27.9 N/mm in MD and 28.6 and 28.4 N/mm in CD, respectively. However, statistically significant differences can be noted between the break properties (*TBS* and *PBE*): the break properties of the GM from the strained area are significantly lower than from the unstrained one, which means that the settlement could induce a reduction of the break properties. For example, the *PYE* for unstrained and strained GM are 1008 and 910% in MD and 998 and 940% in CD, respectively. The settlement would then induce thinning into the geomembrane hence the reduction of break properties.

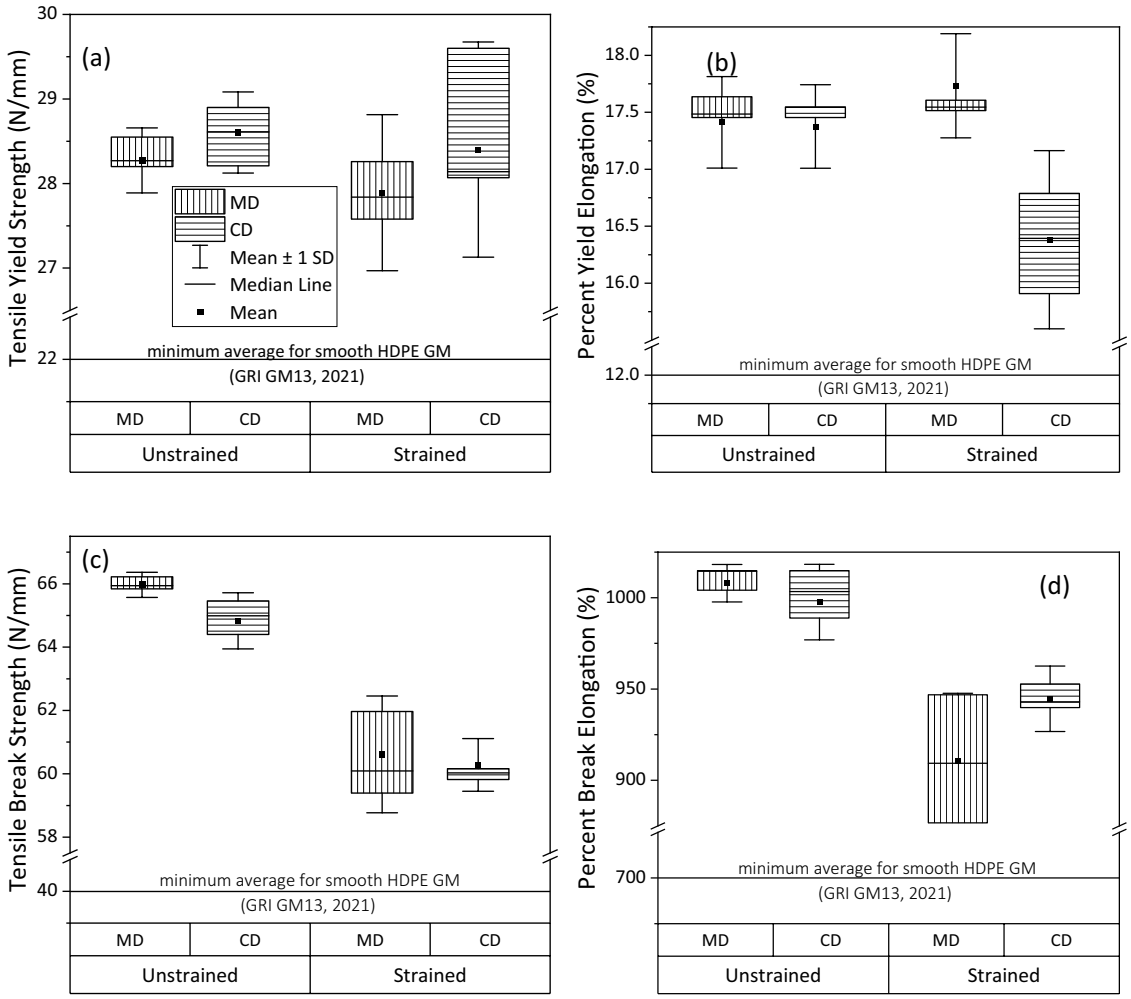

Fig. 6 Box plots (with standard deviations as error bars) of the tensile properties of unstrained and strained GMs in machine (MD) and crossmachine (CD) directions with GRI GM13 [41] minimum requirement: **a** tensile yield stress, **b** percent yield elongation, **c** tensile break strength, and **d** percent break elongation

Table 3 *P* values for the verification of the normality distribution of the tensile properties

Properties	Unstrained		Strained	
	MD	CD	MD	CD
TYS	1.00	1.00	1.00	1.00
PYE	0.50	0.35	0.28	1.00
TBS	1.00	1.00	1.00	1.44
PBE	0.51	1.00	0.99	1.00

Permeability

Figure 7 presents the equivalent hydraulic conductivity (K_g) with the standard error of measurement (*SEM*) determined from preliminary tests as presented in Rarison [16]. The results from the two areas are in the same order of magnitude (10^{-14} m/s). The typical range of K_g values for virgin HDPE GMs is also presented (1.15×10^{-15} m/s $\le K_g \le 1.12\times10^{-14}$ m/s) [51, 59]. The measured K_g values are higher than this range, but they remain around 10^{-14} m/s which means that the GM remains watertight at the two exhumation areas.

Oxygen Sorption and Diffusion Properties

Table 2 presents the oxygen sorption and diffusion properties, i.e., the partitioning coefficient (S_{gf}), diffusion coefficient (D_g), and permeation coefficient (P_g), for the GMs exhumed from the two areas. Figure 8 presents the D_g values (with error bars for the measurements as determined by Rarison [16]) for the GMs from each area (S and U). Typical range of D_g values (1.79×10^{-11} m^2/s $\le D_g \le 3.59\times10^{-11}$ m^2/s) for virgin HDPE films (thickness < 0.250 mm) is also presented [60, 61]. The experimental values of D_g for the

Table 4 Mean comparison of the tensile properties

Properties	Comparison	*p* value	Interpretation
TYS	U-MD vs. U-CD	0.27	Not significantly different
	S-MD vs. S-CD	0.49	Not significantly different
	U-MD vs. S-MD	0.43	Not significantly different
	U-CD vs. S-CD	0.75	Not significantly different
PYE	U-MD vs. U-CD	0.88	Not significantly different
	S-MD vs. S-CD	0.01	Significantly different
	U-MD vs. S-MD	0.27	Not significantly different
	U-CD vs. S-CD	0.04	Significantly different
TBS	U-MD vs. U-CD	0.04	Significantly different
	S-MD vs. S-CD	0.73	Not significantly different
	U-MD vs. S-MD	0.00	Significantly different
	U-CD vs. S-CD	0.00	Significantly different
PBE	U-MD vs. U-CD	0.35	Not significantly different
	S-MD vs. S-CD	0.11	Not significantly different
	U-MD vs. S-MD	0.00	Significantly different
	U-CD vs. S-CD	0.00	Significantly different

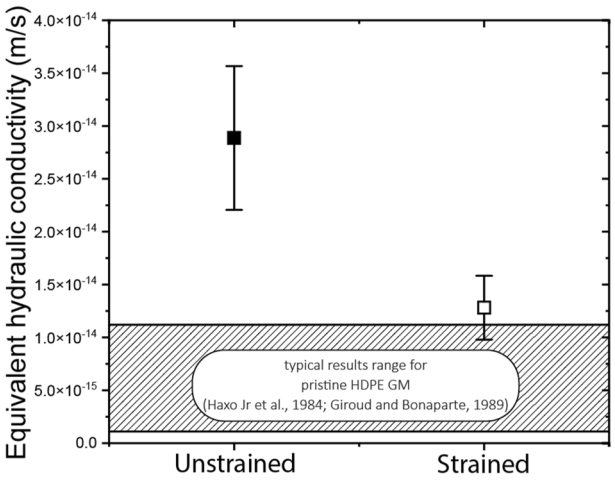

Fig. 7 Equivalent hydraulic conductivity (with error bars) for Unstrained and Strained GMs

strained and unstained GM are close (about 10^{-13} m^2/s) and lower than the typical values given for virgin HDPE films. The exhumed GMs then remain able to limit the oxygen flux.

Conclusions and Limitations

Laboratory tests performed on HDPE GM specimens exhumed from the unstrained and strained areas of a mine site, located in the Mid-North region of Québec, Canada, 20 years after their installation lead to the following conclusions:

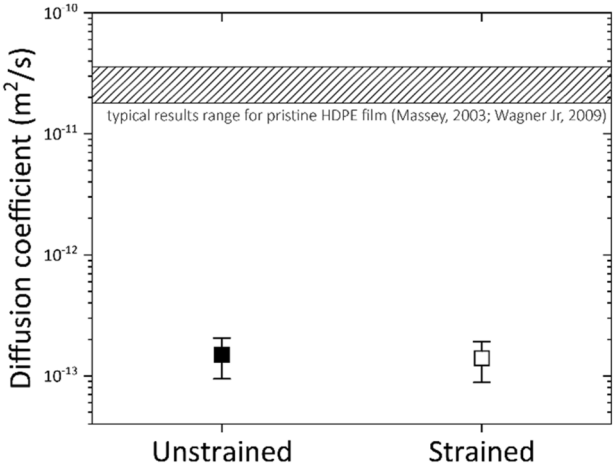

Fig. 8 Oxygen diffusion coefficient D_g (with error bars) for Unstrained and Strained GMs

- The settlement induces thinning into the GM and a loss of mechanical resistance;
- The AO/S have not completely depleted over the 20 years of service, as the measured OITs are above the typical residual values from literature, the GM specimens remain in the first degradation stage of antioxidant depletion;
- The GMs meet almost all GRI GM13 requirements for virgin HDPE GM in terms of chemical and tensile properties even after 20 years of service, except for the HP-OIT;
- The fluid-tightening properties of the GM do not appear to be affected to date as the equivalent hydraulic conductivity values are around 10^{-14} m/s; and the oxygen diffusion coefficients around 10^{-13} m^2/s.

At the scale of the tested samples, the exhumed HDPE GMs do not present visual defects, and they appear to maintain their engineering properties as they remain in the first degradation stage of the degradation model proposed by Hsuan and Koerner [13]. The different conclusions that have been made relate only to the material itself. Further in-service quality controls would be required (every 10 years for example) to monitor potential changes in the GM properties. In the absence of the properties of virgin GM (before installation), the results presented here provide reference values for future works.

This study was performed on small-scale GM samples that would not be representative of the GM at large scale while it is well known that the performance of a GM cover system is significantly affected by the scale. Therefore, field-work at a larger scale should also be necessary to obtain a better understanding of the real performance of GMs used as low permeability layers in cover systems used for the reclamation of mine waste storage facilities. Further

investigations should include assessments of the influence of temperature and settlement on GM strain states as well as the GM water percolation control performance using in-situ data and large-scale infiltration tests.

Acknowledgements The authors would like to acknowledge Professor Ahmed Koubaa for use of the Laboratoire de BIOMATÉRIAUX (Biomaterials Lab) at UQAT. The authors would also like to acknowledge the owner of the Mid-North site for authorizing the use of data. The authors would also like to acknowledge the contribution of the copy editor, Margaret McKyes.

Author Contributions Conceptualization and methodology RFMR, MM and BB; testing, characterization, and analyses RFMR; writing-original draft preparation RFMR; writing-review and editing MM and BB; verification SP; supervision MM and BB.

Funding This study was funded by the Natural Sciences and Engineering Research Council of Canada (NSERC) and the industrial partners of the Research Institute on Mine and Environment (RIME UQAT-Polytechnique: https://irme.ca/en/) through the NSERC-UQAT industrial Chair on Mine Site Reclamation.

Data Availability The datasets generated during and/or analysed during the current study are available from the corresponding author on reasonable request.

Declarations

Conflict of Interest The authors declare that there are no conflicts of interest that could appear to affect the work reported in this paper.

References

1. Lottermoser BG (2010) Mine wastes: characterization, treatment and environmental impacts, 3rd edn. Springer, Berlin, Heidelberg, p 400
2. Plante B, Schudel G, Benzaazoua M (2021) Prediction of acid mine drainage. In: Bussière B, Guittonny M (eds) Hard rock mine reclamation. CRC Press, Boca Raton, pp 21–46
3. Bussière B, Guittonny M (2021) Hard rock mine reclamation: from prediction to management of acid mine drainage. CRC Press, Boca Raton
4. Aubertin M, Bussière B, Pabst T, James M, Mbonimpa M (2016) Review of the reclamation techniques for acid-generating mine wastes upon closure of disposal sites. In: Farid A, De Anirban A, Reddy KR, Yesiller N, Zekkos D (eds) Geosynthetics for sustainable energy. ASCE Library, Chicago, pp 343–358
5. Maqsoud A, Bussière B, Mbonimpa M (2021) Low saturated hydraulic conductivity covers. In: Bussière B, Guittonny M (eds) Hard rock mine reclamation. Boca Raton, CRC Press, pp 93–113
6. Demers I, Pabst T (2021) Covers with capillary barrier effects. In: Bussière B, Guittonny M (eds) Hard rock mine reclamation. Boca Raton, CRC Press, pp 167–186
7. Bussière B, Aubertin M, Chapuis RP (2003) The behavior of inclined covers used as oxygen barriers. Can Geotech J 40(3):512–535. https://doi.org/10.1139/t03-001
8. Yesiller N, Hanson JL, Bussière B, Pabst T, Aubertin M (2018) Use of geomembranes in reclamation covers for reactive mining waste disposal sites." In: 71st Canadian Geotechnical Conference, Edmonton, AB, CA.
9. Müller WW (2007) HDPE geomembranes in geotechnics. Springer, Berlin
10. Scheirs J (2009) A guide to polymeric geomembranes: a practical approach. Wiley, New York
11. Grassie N, Scott G (1985) Polymer degradation and stabilization. Cambridge University Press, New York
12. Scheirs J (2000) Compositional and failure analysis of polymers: a practical approach. Wiley, New York
13. Hsuan Y, Koerner R (1998) Antioxidant depletion lifetime in high density polyethylene geomembranes. J Geotech Geoenviron Eng 124(6):532–541
14. Rollin AL, Lambert S, Pierson P (2002) Géomembranes: guide de choix sous l'angle des matériaux. Presses Inter Polytechnique, Montréal.
15. Koerner RM (2012) Designing with geosynthetics. Xlibris Corporation, United States of America.
16. F. Rarison (2021) Évaluation des propriétés chimiques, mécaniques et hydrogéologiques de géomembranes utilisées comme matériaux de recouvrement pour restaurer des sites miniers en milieu froid et acide, PhD, IRME, Thèse de doctorat, École Polytechnique Montréal, Université du Québec en Abitibi-Témiscamingue.
17. Mbonimpa M, Rarison F, Bussière B, Pouliot S (2021) Utilisation et longevité des géomembranes en restauration des sites miniers. In Symposium 2021 Mines et Environnement, Rouyn-Noranda, QC, CA.
18. Morsy M (2019) Effect of chemical and physical ageing on the longevity of smooth and textured geomembranes in geoenvironmental applications.
19. Gulec S, Benson CH, Edil T (2003) "Effect of acid mine drainage (AMD) on the engineering properties of geosynthetics," presented at the Tailings and Mine Waste. In: Proceedings of the 10th International Conference, Vail, Colorado. pp 12–15.
20. Gulec S, Edil T, Benson C (2004) Effect of acidic mine drainage on the polymer properties of an HDPE geomembrane. Geosynth Int 11(2):60–72
21. Gulec S, Benson C, Edil T (2005) Effect of acidic mine drainage on the mechanical and hydraulic properties of three geosynthetics. J Geotech Geoenviron Eng 131(8):937–950
22. Andersland OB, Ladanyi B (2004) Frozen ground engineering. Wiley, New York
23. MEND (2009) "Mine Waste Covers in Cold Regions, Report 1.61.5a" MEND.
24. MEND (2010) "Cold Regions Cover Research, Report 1.61.5b," MEND.
25. MEND (2012) "Cold regions cover system design technical guidance document, report 1.61.5c." MEND.
26. Lacasse A, Amiri A (1988) "Etude de l'action du gel sur les routes," Ministère des Transports du Québec, Québec, Canada.
27. Martin J, Gardner R (1985) Use of plastics in corrosion resistant instrumentation. Natl Assoc Corros Eng Managing Corros With Plastics 6:126–132
28. Koerner RM, Lord AE, Hsuan YH (1992) Arrhenius modeling to predict geosynthetic degradation. Geotext Geomembr 11(2):151–183. https://doi.org/10.1016/0266-1144(92)90042-9
29. Hsuan Y, et al. (2008) "Long-term performance and lifetime prediction of geosynthetics." In Proceedings of the 4th European Conference on Geosynthetics, Edinburgh, September. Keynote paper.
30. Budiman J (1994) "Effects of temperature on physical behavior of geomembranes." In: Proceedings of the Fifth International Conference on Geotextiles, Geomembranes, and Related Products. International Geosynthetics Society, Easley, South Carolina, USA, Singapore. pp. 1093–1096.
31. Comer AI, Hsuan YG (1996) Freeze-thaw cycling and cold temperature effects on geomembrane sheets and seams. US Department of the Interior, Bureau of Reclamation, Materials

Engineering and Research Laboratory Group, Civil Engineering Services, Technical Service Center.
32. Hsuan Y, Koerner R, Comer A (2013) "Cold Temperature and Freeethaw Cycling Behavior of Geomembranes and their Seams (GSI White Paper 28)." Geosynthetic Institute.
33. McWatters RS, Rutter A, Rowe RK (2016) Geomembrane applications for controlling diffusive migration of petroleum hydrocarbons in cold region environments. J Environ Manag 181:80–94. https://doi.org/10.1016/j.jenvman.2016.05.065
34. Hsuan YG, Koerner RM, Lord AE (1993) Stress-cracking resistance of high-density polyethylene geomembranes. J Geotech Eng 119(11):1840–1855. https://doi.org/10.1061/(ASCE)0733-9410(1993)119:11(1840)
35. Koerner GR, Eith AW, Tanese M (1999) Properties of exhumed HDPE field waves. Geotext Geomembr 17(4):247–261. https://doi.org/10.1016/S0266-1144(98)00024-7
36. Rowe RK, Rimal S, Arnepalli DN, Bathurst RJ (2010) Durability of fluorinated high density polyethylene geomembrane in the Arctic. Geotext Geomembr 28(1):100–107. https://doi.org/10.1016/j.geotexmem.2009.10.012
37. Benson CH, Kucukkirca IE, Scalia J (2010) Properties of geosynthetics exhumed from a final cover at a solid waste landfill. Geotext Geomembr 28(6):536–546. https://doi.org/10.1016/j.geotexmem.2010.03.001
38. Noval A, et al. (2014) "Long-term performance of the HDPE geomembrane at the "San Isidro" reservoir." In: 10th International Conference on Geosynthetics. pp. 427–440.
39. McWatters RS et al (2016) Geosynthetics in Antarctica: Performance of a composite barrier system to contain hydrocarbon-contaminated soil after three years in the field. Geotext Geomembr 44(5):673–685. https://doi.org/10.1016/j.geotexmem.2016.06.001
40. McWatters RS, Rowe RK, Battista VD, Sfiligoj B, Wilkins D, Spedding T (2020) Exhumation and performance of an Antarctic composite barrier system after 4 years exposure. Can Geotech J 57(8):1130–1152. https://doi.org/10.1139/cgj-2018-0715
41. GRI (2021) GM13 Standard specification for test methods, test properties and testing frequency for high density polyethylene (HDPE) smooth and textured geomembranes, GRI, Folsom, PA, United States.
42. Lewis BA, Gallinger RD (1999) "Poirier site reclamation program," in Sudbury '99: mining and the environment II, Sudbury, Ontario, Canada, D. Goldsack, Ed 2:439–448
43. Maurice R (2002) "Restauration du site minier Poirier (Joutel), expériences acquises et suivi des travaux." In: Défis & Perspectives: Symposium 2002 sur l'Environnement et les Mines, Rouyn-Noranda, 3–5 novembre 2002, Rouyn-Noranda, QC, 2002, vol. papier s32 a1021 p545: Développement Économique Canada/Ministère des Ressources Naturelles du Québec/CIM.
44. Rowe RK, Islam M, Hsuan Y (2009) Effects of thickness on the aging of HDPE geomembranes. J Geotech Geoenviron Eng 136(2):299–309
45. ASTM (2019) D5199–12 Standard test method for measuring the nominal thickness of geosynthetics, ASTM, West Conshohocken, PA, United States.
46. ASTM (2019) D3895–19 Standard test method for oxidative-induction time of polyolefins by differential scanning calorimetry, ASTM, West Conshohocken, PA, United States.
47. ASTM (2017) D5885/D5885M, 17 Standard test method for oxidative induction time of polyolefin geosynthetics by high-pressure differential scanning calorimetry, ASTM, West Conshohocken, PA, United States.
48. D6693/D6693M—20 Standard Test Method for Determining Tensile Properties of Nonreinforced Polyethylene and Nonreinforced Flexible Polypropylene Geomembranes, ASTM, West Conshohocken, PA, United States, 2020.
49. AFNOR (2006) NF EN 14150 Détermination de la perméabilité aux liquides, AFNOR, La Plaine Saint-Denis, France.
50. Rarison R, Mbonimpa M, Bussière B (2022) Effects of freeze–thaw cycles on the properties of polyethylene geomembranes. Geosynth Int. https://doi.org/10.1680/jgein.21.00043a
51. Giroud J, Bonaparte R (1989) Leakage through liners constructed with geomembranes—part I. Geomembrane liners. Geotext Geomembr 8(1):27–67
52. Tanaka M, Girard G, Davis R, Peuto A, Bignell N (2001) Recommended table for the density of water between 0 C and 40 C based on recent experimental reports. Metrologia 38(4):301
53. Sangam HP, Rowe RK (2001) Migration of dilute aqueous organic pollutants through HDPE geomembranes. Geotext Geomembr 19(6):329–357
54. Rowe RK, Booker JR (2004) POLLUTE V. 7, 1D pollutant migration through a non-homogeneous soil. Whitby, Ontario, Canada.
55. Student A (1908) The probable error of a mean. Biometrika 6(1):1–25
56. Lilliefors HW (1967) On the Kolmogorov-Smirnov test for normality with mean and variance unknown. J Am Stat Assoc 62(318):399–402
57. Ewais A, Rowe RK (2014) "Degradation of 2.4 mm-HDPE geomembrane with high residual HP-OIT." In: 10th International Conference on Geosynthetics (10th ICG).
58. Ewais AMR, Rowe RK, Scheirs J (2014) Degradation behaviour of HDPE geomembranes with high and low initial high-pressure oxidative induction time. Geotext Geomembr 42(2):111–126. https://doi.org/10.1016/j.geotexmem.2014.01.004
59. Haxo H Jr, Miedema J, Nelson N (1984) Permeability of polymeric membrane lining materials. Technical paper. Matrecon Inc, Oakland
60. Massey LK (2003) Permeability properties of plastics and elastomers: a guide to packaging and barrier materials. Cambridge University Press, Cambridge
61. Wagner JR Jr (2009) Multilayer flexible packaging: technology and applications for the food, personal care, and over-the-counter pharmaceutical industries. Elsevier Science, Amsterdam
62. Landry B, Senay D (2010) Portrait et enjeux miniers de l'Estrie-Version préliminaire du 20 mai 2010. Commission régionale sur les ressources naturelles et le territoire, PRDIRT.
63. Patterson B, Robertson B, Woodbury R, Talbot B, Davis G (2006) Long-term evaluation of a composite cover overlaying a sulfidic tailings facility. Mine Water Environ 25(3):137–145
64. Maurice R (2012) "Normétal mine tailings storage facility HDPE cover: Design considerations and performance monitoring." In: Price WA (ed) 9th International Conference on Acid Rock Drainage, Ontario, ON. Mine Environment Neutral Drainage (MEND).
65. Bradley C, Meiers G, Mayich D, O'Kane M, Shea J (2016) "Use of a conceptual model in advance of numerical simulations to demonstrate an understanding of loading from a reclaimed wate rock pile," presented at the 41st CLRA National Annual General Meeting and Conference. Conference Proceedings, MCIntyre Arena, Timmins, Ontario, June 26–29, 2016, Timmins, ON.
66. Meiers G (2015) "Use of analytical estimates and water balance components to estimate leakage rates through cover systems utilizing a geomembrane," presented at the ACR 2015 October 21-22, 2015. Fredericton, New Brunswick, Canada.
67. Meiers G, O'Kane M, Mayich D, Shea J, Barteaux M (2014) "Evaluation of in service performance of cover systems that utilize a geosynthetic layer," O'Kane Consultant.
68. Meiers G, O'Kane M, Mayich D, Weber P, Bradley C, Shea J (2015) "Closure of legacy waste rock piles: can we achieve passive treatment to manage residual seepage in the short term?" Presented at the 10th International Conference on Mine Closure, June 1–3, 2015, Vancouver, Canada.

69. Cyr J (2011) “Restauration des sites miniers-Présentation du 22 september” MRNF, Québec.
70. MRNF (2009) “Rehabilitation of Site No.1 at the Eustis Mining Complex (Municipalité du Canton de Hatley),” Québec mines, Bulletin d’Information Minière, Juin 2009, vol. Ministère des Ressources Naturelles et Faune, Québec.
71. Turcotte S, Trépanier S, Bussière B (2021) “Restauration des sites miniers abandonnés au Québec : un état de la situation et revue des solutions appliquées,” presented at the Symposium 2021 Mines et Environnement, Rouyn-Noranda, Québec, Canada.
72. Cyr J (2008) “La restauration du site minier Aldermac: un projet de 16,5M$,” presented at the QuébecMines 2008, Bulletin d'information minière, Québec.
73. SNC-Lavalin (2007) “Plan de restauration du site minier Aldermac, Rapport final,” MRNF, Québec.
74. SNC-Lavalin (2010) “Restauration du site minier Aldermac, Rapport tel que construit des travaux effectués en 2008–2009.” MRNF, Québec.
75. Power C et al (2017) Five-year performance monitoring of a high-density polyethylene (HDPE) cover system at a reclaimed mine waste rock pile in the Sydney Coalfield (Nova Scotia, Canada). Environ Sci Pollut Res 24(34):26744–26762. https://doi.org/10.1007/s11356-017-0288-4
76. ECBC (2014) “Former mine site closure program, Update 2013–2014.” Enterprise Cape Breton Corporation.
77. Meiers G, O’Kane M, Mayich D (2012) “Field performance monitoring of a cover system with geosynthetic layers, case study–Franklin waste rock pile, Sydney NS.” O'Kane Consulting.
78. Zetchi M, Fouquet G (2018) “Restauration du site minier abandonné Barvue”. Presented at the QuébecMines, 20–23 Novembre 2018, Québec.
79. MINE_RAGLAN (2015) “Étude d'impact sur l'environnement et le milieu social.” Vol. 1-Rapport principal.

Publisher's Note Springer Nature remains neutral with regard to jurisdictional claims in published maps and institutional affiliations.

Springer Nature or its licensor (e.g. a society or other partner) holds exclusive rights to this article under a publishing agreement with the author(s) or other rightsholder(s); author self-archiving of the accepted manuscript version of this article is solely governed by the terms of such publishing agreement and applicable law.